

# Waiting time distributions of electron transfers through quantum dot Aharonov–Bohm interferometers

Sven Welack,<sup>1,\*</sup> Shaul Mukamel,<sup>2</sup> and YiJing Yan<sup>1,†</sup>

<sup>1</sup>*Department of Chemistry, Hong Kong University of Science and Technology, Kowloon, Hong Kong*

<sup>2</sup>*Department of Chemistry, University of California, Irvine, USA*

(Dated: October 31, 2018)

We present a statistical readout method for quantum interferences based on time series analysis of consecutive single electron transfers through a double quantum dot Aharonov–Bohm interferometer. Waiting time distributions qualitatively indicate the presence of interferences and provide information on orbital-detuning and coherent interdot-electron transfer. Interdot transfer induced oscillations are Aharonov–Bohm phase sensitive, while those due to level detuning are phase-independent. The signature of the quantum interference in the waiting time distribution is more apparent for weakly coupled electron transfer detectors.

PACS numbers: 73.63.Kv, 74.40.+k, 73.23.Hk, 02.50.-r, 03.65.Yz

Double-quantum dot (DQD) junctions provide an experimental setup to study phase coherent transport [1, 2, 3] and to realize Aharonov–Bohm (AB) interferometers [4, 5, 6]. This is of general interest as they are potential candidates for qubits. A crucial aspect for their realization is the noninvasive determination of the presence of quantum interferences in order to minimize decoherence.

So far theoretical studies on transport properties of double quantum dot AB interferometers have been focused on average current [7, 8, 9, 10, 11, 12, 13, 14] and shot noise [15, 16, 17, 18] properties. Recently time-resolved detection of single electron transfers in single quantum dots [19, 20, 21] and DQD in series has become experimentally feasible [22]. Waiting time distributions of consecutive electron transfers can be obtained from time-series analysis and provide detailed information on quantum dots [23, 24] and single molecules [25]. They were found to be sensitive to interference due to multiple electron paths in DQD junctions [23] and contain more detailed information than current and noise measurements [24].

In this letter we propose a weakly invasive statistical method based on waiting time distributions of single external electron transfers that can determine the presence of quantum interferences, small detunings of the DQD orbitals, inter-dot transfer coupling, and Coulomb interaction. These quantities are connected with qualitatively distinguishable oscillations in the waiting time distribution. These oscillations are sensitive to the AB phase,  $\phi = \Phi/\Phi_0$ , and are suppressed at  $\phi = n\pi$  for an integer  $n$  when interdot transfer is present. Here,  $\Phi$  is the magnetic flux perpendicular to the junction and  $\Phi_0 = h/e$  the magnetic flux quanta. In contrast, the oscillations purely due to energy detunings of the DQD orbitals are  $\phi$ -independent. We show that their detection requires

weakly coupled electron detectors thereby avoiding to inflict fast decoherence on the DQD which qualifies the proposed method as a readout scheme for coherently operating qubits.

To that end, we exploit a master equation in the many-body Fock space of the DQD, assuming weak system–reservoir coupling. For simplicity we consider spinless electrons and each QD dot can hold only one electron at most. We decompose the total Hamiltonian of the DQD–AB interferometer junction into  $\tilde{H}_T = \tilde{H}_S + \tilde{H}_R + \tilde{H}_{SR}(\phi)$ . The DQD part (system) reads

$$\tilde{H}_S = \sum_{s=1,2} \epsilon_s c_s^\dagger c_s + U c_1^\dagger c_1 c_2^\dagger c_2 - \Delta (c_1^\dagger c_2 + c_2^\dagger c_1). \quad (1)$$

Here,  $\epsilon_s$  with  $s = 1$  or  $2$  is the orbital energy of the specified QD;  $U$  denotes the strength of the Coulomb repulsion between electrons;  $\Delta$  is the inter-dot electron transfer parameter in the DQD–AB interferometer. The Hamiltonian of the electrodes is given by two independent free electron reservoirs,  $H_R = \sum_{\nu=l,r} \sum_q \epsilon_{q\nu} c_{q\nu}^\dagger c_{q\nu}$ . The index  $\nu$  denotes the left ( $l$ ) or right ( $r$ ) electrode,  $q$  their intrinsic degrees of freedom. The electron creation (annihilation) operators  $c_s^\dagger$  and  $c_{q\nu}^\dagger$  ( $c_s$  and  $c_{q\nu}$ ) satisfy the anticommutator relations:  $\{c_k, c_{k'}^\dagger\} = \delta_{kk'}$  and  $\{c_k^\dagger, c_{k'}^\dagger\} = \{c_k, c_{k'}\} = 0$ , for all  $k, k' = s, q\nu$ . The system–reservoirs coupling responsible for electron transfer between the electrodes and the DQD reads

$$\tilde{H}_{SR}(\phi) = \sum_{\nu=l,r} \sum_{sq} \left[ T_{qs}^{(\nu)}(\phi) c_s^\dagger c_{q\nu} + \text{H.c.} \right]. \quad (2)$$

The AB phase-dependent transfer parameters satisfy  $T_{q1}^{(\nu)}(\phi) = T_{q1} e^{i\phi_\nu/2}$  and  $T_{q2}^{(\nu)}(\phi) = T_{q2} e^{-i\phi_\nu/2}$  for the two parallel dots pierced by a magnetic flux considered here, with  $\phi_l = -\phi_r = \phi$  to account for the sign change in the phase between coupling to left and right electrode.

We describe the DQD by the reduced density operator  $\rho(t)$  of the system. Note that the inter-dot electron transfer  $\Delta$  in Eq. (1) leads to off-diagonal elements in the system Hamiltonian  $\tilde{H}_S$  in the orbital basis. We transform it

\*Electronic address: wesv@ust.hk

†Electronic address: yyan@ust.hk

into eigenbasis,  $H_S = O^{-1} \tilde{H}_S O$ , where  $O$  consists of the eigenvectors of  $\tilde{H}_S$ . The same transformation is applied to the creation and annihilation operators  $\Psi_s = O^{-1} c_s O$  and  $\Psi_s^\dagger = O^{-1} c_s^\dagger O$ , so that  $H_{SR} = O^{-1} \tilde{H}_{SR} O$ . The standard perturbation theory leads to the quantum master equation [23]:

$$\dot{\rho}(t) = -i\mathcal{L}\rho(t) + \sum_{\nu=l,r} (-\Pi_\nu + \Sigma_\nu^+ + \Sigma_\nu^-) \rho(t). \quad (3)$$

The system Liouvillian  $\mathcal{L} = [H_S, \cdot]$  describes the coherent dynamics. The dissipative superoperator in Eq. (3) is separated into the diagonal contribution  $\Pi_\nu$  that leaves the number of electrons in the system unchanged, and the off-diagonal  $\Sigma_\nu^+$  and  $\Sigma_\nu^-$  for the increase and decrease the number of electrons in the DQD, respectively; see Ref. 23 for the derivation. This separation is necessary in order to keep track of the trajectories of single electron transfers. Consider, for example, the scenario of detecting an electron entering the DQD through the left electrode at time  $t_0$  and leaving through the right electrode at time  $t$ . The waiting-time distribution of consecutive electron transfer events is then given by the joint-probability [23]:

$$P_{l \rightarrow r}(t, t_0) = \text{tr}_S \{ \Sigma_r^- S_{t, t_0} \Sigma_l^+ \rho_S(t_0) \}, \quad (4)$$

with  $S_{t, t_0} = \exp[(-i\mathcal{L} - \Pi_l - \Pi_r)(t - t_0)]$  being the propagator of the system in the absence of transfer events at the electrodes within the waiting time interval. Quantity (4) can be obtained from the time-series of single directionally resolved electron transfers between the electrodes and the system. One has to record a sufficiently large number of the  $l \rightarrow r$  events and generate a histogram of the number of occurrences as function of the time interval  $t - t_0$ . The histogram has to be normalized by the total number of considered events.

The aforementioned physically distinct dissipative components are formally given as [23]:  $\Sigma_\nu^+ = \sum_s \vec{\Psi}_s^\dagger \vec{\Psi}_{\nu s}^{(-)} + \vec{\Psi}_s \vec{\Psi}_{\nu s}^\dagger^{(-)}$ ,  $\Sigma_\nu^- = \sum_s \vec{\Psi}_s^\dagger \vec{\Psi}_{\nu s}^{(+)} + \vec{\Psi}_s \vec{\Psi}_{\nu s}^\dagger^{(+)}$ , and  $\Pi_\nu = \sum_s (\vec{\Psi}_s^\dagger \vec{\Psi}_{\nu s}^{(+)} + \vec{\Psi}_s \vec{\Psi}_{\nu s}^\dagger^{(-)} + \text{H.c.})$ . The involved superoperators are defined as the left- or right-actions ( $\vec{\Psi} \cdot \equiv \vec{\Psi} \cdot$  or  $\vec{\Psi} \cdot \equiv \cdot \vec{\Psi}$ ) of the associated Hilbert-space  $\Psi$ -operators. Besides the annihilation (creation) operators  $\Psi_s$  ( $\Psi_s^\dagger$ ) we also have to consider their auxiliaries [23, 26]:

$$\Psi_{\nu s}^{(\pm)}(t, \phi) = \sum_{s'} \int_{t_0}^t dt' C_{\nu s s'}^{(\pm)}(t - t'; \phi) e^{-i\mathcal{L}(t-t')} \Psi_{s'}. \quad (5)$$

Here,  $C_{\nu s s'}^{(+)}(t; \phi) = \sum_{q q'} T_{q s}^{(\nu)*}(\phi) T_{q' s'}^{(\nu)}(\phi) \langle c_{q\nu}^\dagger(t) c_{q'\nu}(0) \rangle_R$  and  $C_{\nu s s'}^{(-)}(t; \phi) = \sum_{q q'} T_{q s}^{(\nu)}(\phi) T_{q' s'}^{(\nu)*}(\phi) \langle c_{q\nu}(t) c_{q'\nu}^\dagger(0) \rangle_R$  are the AB phase-dependent interacting reservoir correlation functions. Applying the given phase relations in  $T_{q s}^{(\nu)}(\phi)$  and assuming further  $T_{q1} = T_{q2} = T_q$  for the AB phase-free parts lead to the relations:  $C_{\nu 11}^{(\pm)}(t) = C_{\nu 22}^{(\pm)}(t) = C_\nu^{(\pm)}(t)$ ,  $C_{\nu 12}^{(\pm)}(t) = C_\nu^{(\pm)}(t) e^{i\phi_\nu}$ , and  $C_{\nu 21}^{(\pm)}(t) = C_\nu^{(\pm)}(t) e^{-i\phi_\nu}$ . The auxiliary operators in

their non-Markovian form [Eq. (5)] can be numerically evaluated numerically without further approximations as shown in Ref. 23 and 26.

To derive analytical results we apply the Born-Markov approximation, together with the wide-band limit for the reservoir spectral density. The latter leads to  $C_\nu^{(\pm)}(t) = \Gamma \int_0^\infty d\epsilon f_\nu^{(\pm)}(\epsilon) e^{\mp i\epsilon t}$ . Here,  $f_\nu^+(\epsilon) = 1 - f_\nu^-(\epsilon) = [e^{\beta(\epsilon - \mu_\nu)} + 1]^{-1} \equiv f(\epsilon - \mu_\nu)$  is the Fermi distribution function, with  $\beta$  being the inverse temperature and  $\mu_\nu$  the Fermi energy of the electrode  $\nu$ . The Born-Markov approximation amounts to replacing the range of time integration in Eq. (5) with  $(-\infty, \infty)$ . As results, the auxiliary annihilation operators defined in Eq. (5) can be evaluated as

$$\Psi_{\nu 1}^{(\pm)} = \Gamma f_\nu^\pm(\mathcal{L})(\Psi_1 + \Psi_2 e^{\pm i\phi_\nu}), \quad (6a)$$

$$\Psi_{\nu 2}^{(\pm)} = \Gamma f_\nu^\pm(\mathcal{L})(\Psi_1 e^{\mp i\phi_\nu} + \Psi_2), \quad (6b)$$

which depend on the AB-phase ( $\phi = \phi_l = -\phi_r$ ) but no long on the time. The auxiliary creation operators  $\Psi_{\nu s}^{\dagger(\pm)}$  are of similar expressions, but with the replacements of  $\mathcal{L} \rightarrow -\mathcal{L}$ ,  $\phi \rightarrow -\phi$  and  $\Psi_s \rightarrow \Psi_s^\dagger$  in Eq. (6). Note that since  $H_S$  is diagonal in the many-body Fock space, the action of the superoperator  $f_\nu^\pm(\mathcal{L})$ , which is determined by the Fermi function and the diagonal system Liouvillian, can be carried out easily. All the 16 auxiliary operators,  $\Psi_{\nu s}^{(\pm)}$  and  $\Psi_{\nu s}^{\dagger(\pm)}$  with  $\nu = l, r$  and  $s = 1, 2$ , can now be evaluated [cf. Eq. (6)] in terms of  $4 \times 4$  matrices in the Fock-space representation. Consequently, the action of each dissipative tensor in the second term of Eq. (3), which has been given in terms of the left- and right-multiplications of some  $\Psi_s$  ( $\Psi_s^\dagger$ ) and  $\Psi_{\nu s}^{(\pm)}$  ( $\Psi_{\nu s}^{\dagger(\pm)}$ ) is now determined. It is worth to mention here that the approximation scheme explored in Eq. (6) leads to an Eq. (3) in Lindblad form.

We use the following parameter scheme to describe our calculation results. A bias of  $2V$  is applied symmetrically  $\mu_{l/r} = \mu_{\text{eq}} \pm V$ . The orbital energies of the DQD are set to be  $\epsilon_1 = \epsilon_g + \alpha$  and  $\epsilon_2 = \epsilon_g - \alpha$ ; i.e., the orbital energy split (or detuning) is  $2\alpha$ . We set the vacuum DQD state  $\epsilon_0 = 0$  as the energy zero, and  $\epsilon_g = 1$  the internal energy unit. In all calculations,  $\mu_{\text{eq}} = 1.0$  and  $T = 0.1$ .

Figure 1 demonstrates the dependence of the waiting time distributions  $P_{l \rightarrow r}(t)$  (left-panels) on the AB-phases  $\phi$ , together with their Fourier transforms  $F(\omega)$  (right-panels) exemplified at three representing values of  $\phi = 0, \pi/2$ , and  $\pi$ . The Coulomb repulsion parameter  $U = 1.0$  and the bias  $2V = 0.2$  are common, while the interdot transfer and orbital energy split parameters are  $(\Delta, \alpha) = (0.1, 0)$  in the upper,  $(0, 0.05)$  in the middle, and  $(0.1, 0.05)$  in the bottom panels, respectively. Clearly, the influences of  $\Delta$  and  $\alpha$  on the waiting time distribution are *qualitatively* distinct, especially in the two limiting regimes. While  $P_{l \rightarrow r}(t)$  shows only little dependence on  $\phi$  in the dot orbital-split case (the middle panel:  $\Delta = 0$  but  $\alpha \neq 0$ ), it is strikingly sensitive to the AB-phase in the interdot-transfer case (the upper panel:  $\Delta \neq 0$  but

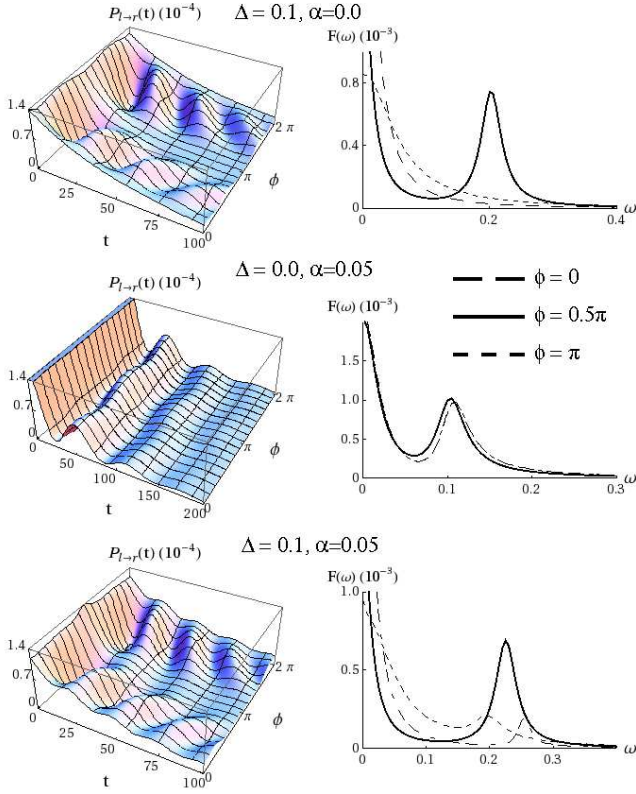


FIG. 1:  $P_{l \rightarrow r}(t)$  (left-panels) as functions of AB-phase  $\phi$  and time  $t$ ; The corresponding Fourier transformation  $F(\omega)$  (right-panels) at  $\phi = 0$  (dash),  $\pi/2$  (solid), and  $\pi$  (dot), respectively. The upper, middle and bottom panels are for three representing sets of interdot-transfer rate  $\Delta$  and orbital detuning  $\alpha$ . Other parameters are  $U = 1.0, T = 0.1, 2V = 0.2$  and  $\mu_{\text{eg}} = 1.0$  (in unit of  $\epsilon_g$ ); see text for details.

$\alpha = 0$ ). In the latter case, the characteristic oscillation is maximized at  $\phi = \pi/2$ , but disappears at  $\phi = 0$  and  $\phi = \pi$ . These observations can be largely understood as follows.

The dot orbital-split ( $\Delta = 0$  but  $\alpha \neq 0$ ) case resembles the transport through double slits. The resulting interference [23] persists and is insensitive to the AB phase, due to the fact that  $\phi_l = -\phi_r$  in each orbital channel largely cancels out the AB-phase effect. This accounts for the basic feature observed in the middle panels of Fig. 1.

In interdot-transfer case (upper panels:  $\Delta \neq 0$  but  $\alpha = 0$ ), the aforementioned double-slit feature is destroyed. The interdot-transfer allows electrons to switch between the two pathways provided by the DQD. Thus, different phases can be accumulated as the electron transfer through the coupled DQD and the aforementioned phase symmetry is broken along some of the possible transfer trajectories. As a result, the total accumulated phase depends on the value of  $\phi$ . It leads to a pure decay of  $P_{l \rightarrow r}(t)$  at the AB phase  $\phi = 0$  or  $\pi$ , where  $e^{i\phi} = e^{-i\phi}$ . However, at other values of  $\phi$ , it leads to an effective phase difference between the eigen-levels which are sub-

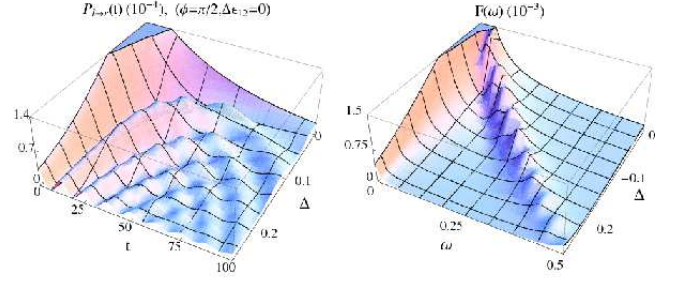


FIG. 2:  $P_{l \rightarrow r}(t)$  as function of inter-dot transfer rate  $\Delta$  and time  $t$  and corresponding Fourier transformation  $F(\omega)$ . The AB-phase is  $\phi = \pi/2$  and the orbital detuning  $\alpha = 0$ . Other parameters are same as Fig. 1.

ject to an induced energy gap of  $2\Delta$ , responsible for the AB-phase activated oscillations observed in the upper panels of Fig. 1.

In the intermediate regime shown in the bottom panels of Fig. 1, oscillations can be observed for all  $\phi$ ; however, the Fourier transform reveals a frequency shift when AB-phase is tuned by the magnetic field. At  $\phi = \pi/2$ , the observed frequency corresponds to the DQD eigenenergy gap ( $2\sqrt{\Delta^2 + \alpha^2} = 0.224$ ), while at  $\phi = 0$  or  $\pi$ , it is blue or red shifted, respectively. The amplification of the oscillation at  $\phi = \pi/2$  is characteristic for inter-dot transfer and allows to distinguish it from orbital detuning. The latter causes only small oscillations at  $\phi = 0$  or  $\pi$ .

Figure 2 examines further the influence of  $\Delta$  on  $P_{l \rightarrow r}(t)$  (left) and its spectrum  $F(\omega)$  (right), with  $\alpha = 0$  and  $\phi = \pi/2$ , where oscillations due to AB phase-activated interferences between the eigen-levels are at maximum. Note that the interference would remain dark at  $\phi = 0$  in this case; as can be seen the upper panels of Fig. 1. The amplitude of  $P_{l \rightarrow r}(t)$  oscillation decreases with  $\Delta$ , which corresponds to a decreased average current through the DQD.

To analyze other coherent operation conditions, let us focus on the orbital-detuning ( $\Delta = 0$  and  $\alpha \neq 0$ ) case where  $\tilde{H}_S$  is diagonal. We also neglect the Liouville-space off-diagonal elements in  $\Pi_l + \Pi_r$ , which have a relatively small influence in the weak coupling regime. As results, the propagator  $S_{t,t_0}$  in determining  $P_{l \rightarrow r}(t, t_0)$  [Eq. (4)] becomes diagonal, and the analytical solution is achievable. Moreover, the waiting time distribution is separable into  $P_{l \rightarrow r}(t) = P_{\text{osc}}(t) + P_{\text{decay}}(t)$ . A detailed discussion of the decaying terms  $P_{\text{decay}}(t)$  that depends weakly on the AB-phase would exceed the scope of this letter; but it has been provided for the case of incoherent transport through single benzene molecules [25] which can be applied to QD-systems as well. As the coherent operation conditions are concerned, we focus only on the oscillation term, which is independent of the AB-phase for the orbital-split case (cf. the middle panels of Fig. 1).

$$P_{\text{osc}}(t) = p_0 \Gamma^2 b^2(V, \alpha) e^{-2a(U, V) \Gamma t} \cos(2\alpha t), \quad (7)$$

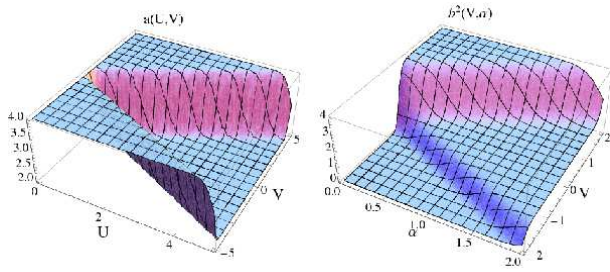


FIG. 3: The damping parameter  $a(U, V)$  and the pre-exponential amplitude parameter  $b^2(V, \alpha)$ , as their function dependence, for the oscillation term  $P_{osc}(t)$  [Eq. (7)]. Inter-dot electron transfer is absent  $\Delta = 0$ .

where  $p_0$  is the initial vacuum state occupation number,  $a(U, V) = a(U, -V) = f(U + V) + f(U - V) + 2$ , and

$$b(V, \alpha) = \frac{1 + e^{2\alpha\beta} + 2e^{(V+\alpha)\beta}}{e^{\beta(V+2\alpha+1)/2}} f(V + \alpha) f(V - \alpha). \quad (8)$$

The left-panel of Fig. 3 depicts the damping parameter  $a$  as function of  $U$  and  $V$ . It assumes the maximum value of 4 for small Coulomb coupling  $U < V$  and is independent of  $\alpha$ . Also the decay rate proportional to the system-electrode coupling strength  $\Gamma$ . Thus a weak coupling is required for the observability of interferences. This qualifies statistical analysis of waiting time distributions as an indirect method to study internal processes indirectly avoiding fast decoherence in the system.

The right-panel of Fig. 3 depicts the pre-exponent parameter  $b^2$  as function of  $V$  and  $\alpha$ . It reveals further the parameter regimes where oscillations are observable. One condition is that  $V < \alpha$ . Oscillations are suppressed at negative bias larger than the DQD energy gap. The amplitude is strongly increased when  $V > \alpha$ . However in this regime the decay rate  $2\alpha\Gamma$  may reach its maximum and prevent the observability of coherence. Apparently,

the presence of strong Coulomb coupling, as well as operating at small bias regime, are favored for the observation of interference effects by means of waiting time distributions.

In conclusion, a Markovian quantum master equation in the Fock space was formulated and employed to calculate the waiting time distribution of consecutive electron transfers in AB interferometers. Based on this we describe a novel statistical method to determine quantum interferences, inter-dot electron transfers, orbital detuning and the AB-phase. Orbital detuning and inter-dot transfer induce oscillations in the waiting time distribution in the presence of interference. The two cases can be distinguished qualitatively since the latter one is sensitive to the AB-phase. The observability of oscillations requires the presence of strong Coulomb interaction, small bias and a weak electrode-system coupling.

The indirectness of the statistical detection avoids fast decoherence but a large number of transfer events is necessary in order to extract information. This might be advantageous for a qubit in operation with a continuous readout. The method does not provide information on a single operation but can determine whether a large set of operations is carried out coherently. Also other sources of decoherence like coupling to phonon bath have to be minimized. The signature of interferences in waiting time distribution can survive in the presence of a phonon-bath [24]. The proposed scheme can be realized utilizing presently available technology. For that purpose two DQD in series junctions which act as detectors by their coupling to their respective quantum point contacts [22] should be installed on both sides of a parallel DQD junction. This setup consisting of six QDs avoids decoherence inflicted by the charge state measurement of the quantum point contact.

Support from the RGC (604007 & 604508) of Hong Kong (to YJY), NSF (CHE-0745892/CBC-0533162) and NIRT (EEC 0303389) of USA (to SM) is acknowledged.

- 
- [1] F. R. Waugh et al., Phys. Rev. Lett. **75**, 705 (1995).
  - [2] J. C. Chen, A. M. Chang, and M. R. Melloch, Phys. Rev. Lett. **92**, 176801 (2004).
  - [3] A. W. Holleitner, R. H. Blick, A. K. Hüttel, K. Eberl, and J. P. Kotthaus, Science **297**, 70 (2002).
  - [4] A. W. Holleitner, C. R. Decker, H. Qin, K. Eberl, and R. H. Blick, Phys. Rev. Lett. **87**, 256802 (2001).
  - [5] T. Ihn, M. Sigrist, K. Ensslin, W. Wegscheider, and M. Reinwald, New Journal of Physics **9**, 111 (2007).
  - [6] M. Sigrist, T. Ihn, K. Ensslin, D. Loss, M. Reinwald, and W. Wegscheider, Phys. Rev. Lett. **96**, 036804 (2006).
  - [7] V. M. Apel, M. A. Davidovich, G. Chiappe, and E. V. Anda, Phys. Rev. B **72**, 125302 (2005).
  - [8] V. Moldoveanu, M. Tolea, A. Aldea, and B. Tanatar, Phys. Rev. B **71**, 125338 (2005).
  - [9] L. G. Mourkh and A. Y. Smirnov, Phys. Rev. B **72**, 033310 (2005).
  - [10] P. Simon and D. Feinberg, Phys. Rev. Lett. **97**, 247207 (2006).
  - [11] Y. Tokura, H. Nakano, and T. Kubo, New Journal of Physics **9**, 113 (2007).
  - [12] F. Li, X. Q. Li, W. M. Zhang, and S. A. Gurvitz, "Magnetic field switching in parallel quantum dots", arxiv:0803.1618.
  - [13] K. Kang and S. Y. Cho, J. Phys.: Condens. Matter **16**, 117 (2004).
  - [14] B. Kubala and J. König, Phys. Rev. B **65**, 245301 (2002).
  - [15] D. Loss and E. V. Sukhorukov, Phys. Rev. Lett. **84**, 1035 (2000).
  - [16] G. B. Zhang, S. J. Wang, and L. Li, Phys. Rev. B **74**, 085106 (2006).
  - [17] B. Dong, X. L. Lei, and N. J. M. Horing, Phys. Rev. B

- 77**, 085309 (2008).
- [18] J. Peng, B. Wang, and D. Y. Xing, Phys. Rev. B **71**, 214523 (2005).
  - [19] W. Lu, Z. Ji, L. Pfeiffer, K. W. West, and A. J. Rimberg, Nature **423**, 422 (2003).
  - [20] T. Fujisawa, T. Hayashi, Y. Hirayama, and H. D. Cheong, Appl. Phys. Lett. **84**, 2343 (2004).
  - [21] S. Gustavsson et al., Phys. Rev. Lett. **96**, 076605 (2006).
  - [22] T. Fujisawa, T. Hayashi, R. Tomita, and Y. Hirayama, Science **312**, 1634 (2006).
  - [23] S. Welack, M. Esposito, U. Harbola, and S. Mukamel, Phys. Rev. B **77**, 195315 (2008).
  - [24] T. Brandes, Ann. Phys. **17**, 477 (2008).
  - [25] S. Welack, J. B. Maddox, M. Esposito, U. Harbola, and S. Mukamel, Nano Lett. **8**, 1137 (2008).
  - [26] S. Welack, M. Schreiber, and U. Kleinekathöfer, J. Chem. Phys. **124**, 044712 (2006).